

Prediction of charge separation in GaAs/AlAs cylindrical nanostructures

Jeongnim Kim, Lin-Wang Wang, and Alex Zunger
National Renewable Energy Laboratory, Golden, Colorado 80401
-Received 13 August 1997!

It is known that in a sequence of flat, type-I $(\text{GaAs})_m/(\text{AlAs})_n/(\text{GaAs})_p/(\text{AlAs})_q \dots$ multiple quantum wells (MQWs), the wave functions of both the valence-band maximum and the conduction-band minimum are localized on the widest well. Thus, electron-hole charge separation is not possible. On the other hand, for short-period superlattices (type II), the electron and hole are localized on different materials (electron on AlAs and hole on GaAs) and different band-structure valleys (hole at G and electron at X). Using a plane-wave pseudopotential direct-diagonalization approach, we predict that electron-hole charge separation on different layers of the *same* material (GaAs) and *same* valley (G) is possible in *curved* (but not in flat) geometries. This is predicted for a set of concentric, nested cylinders of GaAs and AlAs (Russian Doll). Since the flat multiple-quantum-well structure and the Russian Doll structure with the same layer thicknesses have the same band offset diagram, the difference in behavior is not due to the potential. Rather, it reflects different interband coupling and kinetic energy confinement induced by the *curvature*, present in the nested-cylinder geometry but absent in the MQW. This identifies a geometric degree of freedom (curvature) that can be used to tailor electronic properties of nanostructures. #0163-1829-97151644-4#

Recent advances in nanotechnology permit fabrication of complex nanostructures with special electronic and optical properties reflecting dimensional confinement on a nanometer scale,^{1,2} e.g., multiple quantum wells³ and core-shell structures.⁴ The essential building blocks of such structures are alternating layers of different semiconducting materials, acting as “wells” and “barriers,” and controlling the confinement energies and thus the localization of charge carriers. The materials comprising the wells and barriers are usually flat, two-dimensional semiconductor films,³ stacked like a deck of cards to produce “multiple quantum wells (MQWs)” or “superlattices.” In this case, wave functions of the conduction-band minimum (CBM) and valence-band maximum (VBM) at the Brillouin zone center, are localized on the *widest wells*, having the lowest confinement energy.^{3,5} Consequently, it is normally impossible to create a sequence of flat layers that would exhibit separation of charge carriers on different layers of the *same material*. When electron-hole charge separation does exist, it is found that the electron and the hole are localized on *different materials*, as in “type-II” superlattices⁶ (e.g., electrons in AlAs and holes in GaAs). Similarly, “charge transfer” transitions in inorganic solids⁷ involve localization of electrons and holes on different atoms or chemical groups within the solid (e.g., on the ligand and on the core metal, respectively). Since nonplanar geometry of multiple-quantum wells, envisioned by Watanabe⁸ and discussed by Tatarinova *et al.*⁹, are now realized via “core-shell structures,”⁴ we were wondering if utilization of such distinct geometric degrees of freedom could affect charge separation of electrons and holes on different layers of the *same material* (e.g., GaAs).

We have thus contrasted the quantum confinement of (i) multiple quantum wells of *flat* GaAs and AlAs layers, i.e., $(\text{GaAs})_m/(\text{AlAs})_n/(\text{GaAs})_p/(\text{AlAs})_q$, with (ii) nested cylinders—an equivalent sequence of wells and barriers arranged as *concentric wires* (Russian Doll) (Fig. 1). Using a pseudopotential plane-wave calculation, we identified a set of periods (

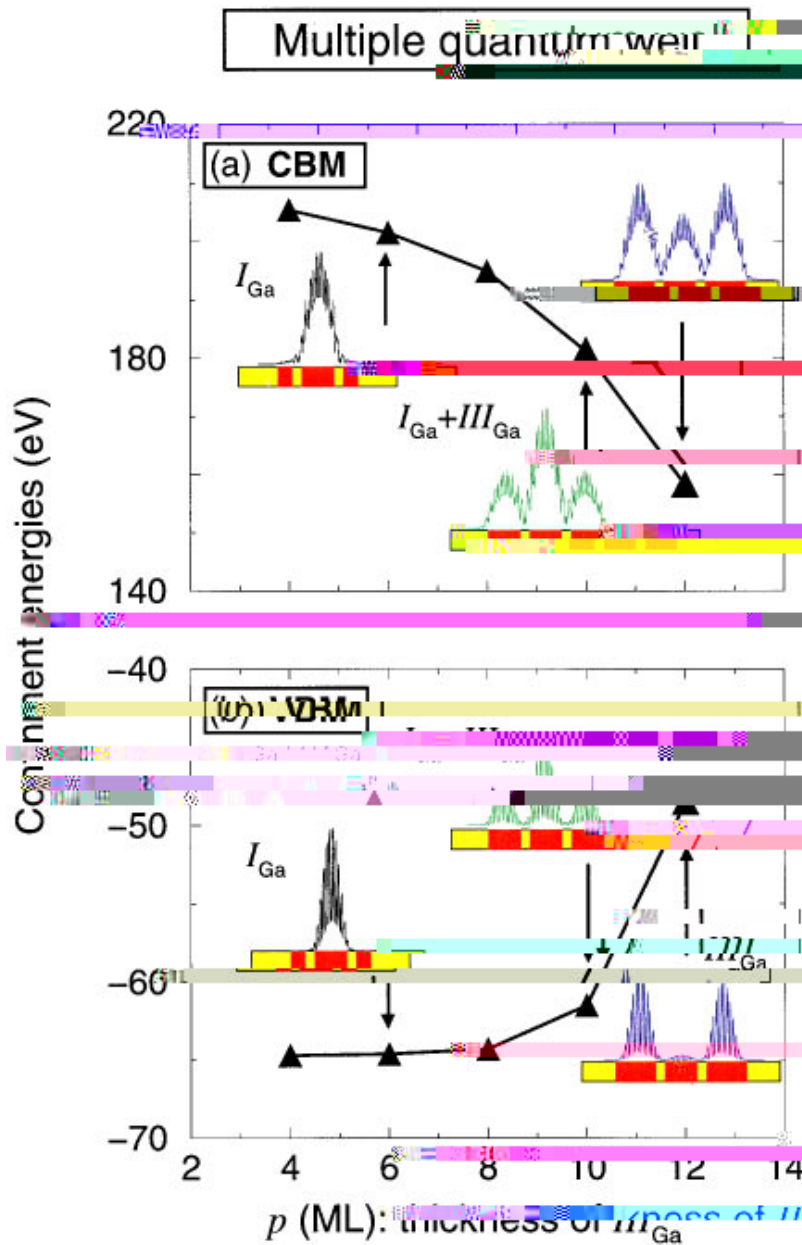


FIG. 2. Confinement energies

study thus identifies a new geometric degree of freedom ~curvature! that can be used to manipulate electronic properties of nanostructures.¹⁰

The electronic structure of the nanostructures is described here using a direct-diagonalization ~multiband! approach to the single-particle Schrödinger equation,

$$\left\{ \sum_{na} \frac{1}{2} v_a(\mathbf{r} - \mathbf{d}_a) \delta(\mathbf{r} - \mathbf{d}_a) \right\} c_i(\mathbf{r}) = \epsilon_i c_i(\mathbf{r}), \quad (1)$$

where v_a is the screened pseudopotential of atom of type a located at site \mathbf{d}_a within cell \mathbf{R}_n . The pseudopotential is fit to the measured bulk band structures and to the *ab initio* bulk wave functions.¹¹ The potential used here accurately describes type-I/type-II transitions in ordered AlAs/GaAs superlattices⁶ as well as the bowing in bulk $\text{Al}_x\text{Ga}_{1-2x}\text{As}$

random alloys¹¹ and wave function localization in disordered superlattices.¹² We use the “folded spectrum method”,¹³ to find the band edge eigenstates of Eq. (1). Its linear scaling with the number of atoms allows us to handle easily systems of $10^3 - 10^4$ atoms.

Figure 2 shows the calculated confinement energies of the conduction-band minimum and the valence-band maximum of *linear multiple quantum wells* as a function of the thickness $p(\text{III}_{\text{Ga}})$ of the outer GaAs segment ~see Fig. 1 for a definition of the structure!. Confinement energies are defined with respect to CBM and VBM of bulk GaAs. The thickness of the innermost GaAs segment is fixed at $m(I_{\text{Ga}}) \approx 5$ monolayers ~ML!. Figure 2 also shows the wave function amplitudes of the nanostructures, so that the localization can be assessed. The red bars denote AlAs layers, while the yellow

bars denote GaAs layers. We see that, as expected, both the CBM and VBM are localized on the widest wells. Wave functions are localized on the innermost GaAs segment (I_{Ga}) when layer III_{Ga} is below 10 ML. They are localized on the III_{Ga} segment when layer III is thicker than the innermost layer, i.e., $p > 2m$. When the two GaAs wells, I_{Ga} and III_{Ga} , have the same thickness, $p = 2m$

of the two valence states (triangles and circles in Fig. 4-b) cross. The two valence states of the nested cylinders in Fig. 3-b) have different nodal structures and angular momenta: In cylindrical coordinates (r, ϕ, z) , we can express the valence wave functions in terms of bulk wave functions at Brillouin zone center (u_i where $i = x, y, z$) and envelope functions $e^{im_z \phi} f_{m_z}(r)$. Under spherical approximation of the bulk Hamiltonian, the wave functions marked in Fig. 3-b) by triangles can be written as $u_z f_0(r)$, where $m_z = 0$. Thus, $f_0(r)$ has its *maximum* at the center $r = 0$. On the other hand, the wave functions marked in Fig. 3-b) by circles can be expressed as $(u_x \pm i u_y) e^{i\phi} f_1(r)$. The angular momentum of this state constrains the amplitude of $f_1(r)$ to be *zero* at $r = 0$ and introduces a centrifugal potential proportional to m_z^2/r^2 with $m_z = 1$. Therefore, the valence states with $m_z = 1$ favors localization far from the center, while the state with $m_z = 0$ lacks any centrifugal potential, so it localizes at the center. Note that, both the states marked in Fig. 3-b) by triangle and circle have a zero z component of the total angular momentum. Thus, they are both singlet states. Charge separation occurs when the thickness $p(\text{III}_{Ga})$ is large enough so that the kinetic confinement